Synthesis, Molecular Structures, and Properties of Six-Coordinate $[Fe(OEP)(L)(NO)]^+$ Derivatives: Elusive Nitrosyl Ferric Porphyrins

Mary K. Ellison and W. Robert Scheidt*

Contribution from The Department of Chemistry and Biochemistry, University of Notre Dame, Notre Dame, Indiana 46556

Received December 14, 1998

Abstract: The preparation and characterization of several $\{FeNO\}^6$ porphyrinates ($[Fe(OEP)(L)(NO)]^+$), where OEP is octaethylporphyrin and L is one of the neutral nitrogen-donating axial ligands 1-methylimidazole (1-MeIm), pyrazole (Pz), indazole (Iz), or pyrazine (Prz), are described. The synthesis and crystallization of these derivatives requires an NO atmosphere and careful attention to conditions. The characterization of these $[Fe(OEP)(L)(NO)]^+$ complexes by IR and UV−vis spectroscopies provides for general distinctions between five- and six-coordination and the two common oxidation states of iron nitrosyl porphyrins. The UV−vis spectra of the $[Fe(OEP)(L)(NO)]^+$ derivatives are all characterized by very distinct α and β bands. The solid-state NO stretching frequencies are found in the narrow range of 1890 to 1921 cm^{-1}. Six X-ray structure determinations have been completed. The molecular structures of $[Fe(OEP)(1\text{-MeIm})(NO)]ClO_4$, $[Fe(OEP)(Pz)(NO)]ClO_4$(**1**), $[Fe(OEP)(Iz)(NO)]ClO_4$, and $\{[Fe(OEP)(NO)]_2Prz\}(ClO_4)_2$ are described in detail. All structural features are consistent with the assignment of a low-spin state to the central iron. The $Fe-N_p$ bond lengths range from 1.995(8) to 2.004(5) Å. The axial $Fe-N_{NO}$ bond lengths are quite short (range 1.627(2)−1.6465(17) Å). The Fe−N−O groups are essentially linear (Fe−N−O angle range is 176.6(3)−177.6(3)°) which is that expected for these $\{FeNO\}^6$ species. The Fe−L bond lengths trans to the nitrosyl are normal (range 1.988(2)−2.039(2) Å); there is no nitrosyl structural trans effect. The iron is displaced only slightly out of the plane of the 24-atom core toward the nitrosyl, and with the short $Fe-N_{NO}$ bond lengths steric interactions cause modest porphyrin core distortions.

Introduction

Although it is now well recognized that nitric oxide (NO) plays an important role in mammalian physiology, especially through its interaction with iron(II) heme proteins, only just recently have several studies shown that iron(III) nitrosyl heme proteins are biologically important. Iron(III) hemes (nitrophorins) have been discovered in the salivary glands of the bloodsucking insects *Rhodnius prolixus* and *Cimex lectularius*.[1,2] Both of these distinctly different nitrophorins can reversibly bind NO without reduction to an iron(II) derivative. The pH-dependent NO binding affinity of these proteins allows both the storage of NO in the bug's salivary glands and the release of NO, in host tissues which induces local vasodilation to aid the bug's blood feeding. $\{FeNO\}^6$ hemes are also thought to be key intermediates in the denitrification processes of bacteria and fungi. One of these intermediates has been proposed in the reduction of nitrite by heme cd_1 nitrite reductase.[3,4] A similar intermediate is also suggested in the reduction of NO to N_2O by fungal *Fusarium oxysporum* cytochrome P450 nitric oxide reductase.[5] Spectroscopic and structural information suggests that some of these $\{FeNO\}^6$ heme intermediates are six-coordinate species with neutral nitrogen-donating axial ligands such as histidine trans to the nitrosyl.[6,7] These newly discovered interactions of NO with iron(III) hemes underscore the importance of further study of ferric nitrosyl porphyrin complexes.

The electron-counting formalism and notation of Enemark and Feltham will be used throughout this paper.[8,9] The formalism and notation considers the MNO group as a strongly covalently bonded unit in which properties and structure can be anticipated from a knowledge of the number of electrons in the unit written as $\{MNO\}^n$. The total number of electrons (n in the notation) is the number of d electrons from the metal, always evaluated by considering NO as neutral, plus the one unpaired electron from the π^* orbitals of neutral NO. Species denoted as $\{FeNO\}^6$ can thus be regarded as being derived from iron(III) centers and NO, while the $\{FeNO\}^7$ species are regarded as being derived from iron(II) centers and NO. We have attempted to avoid specification of the usual formal oxidation states; again the $\{FeNO\}^6$ and $\{FeNO\}^7$ notation is used to emphasize the strongly covalent and delocalized nature of the three-atom group. Prior investigations led us to expect that the $\{FeNO\}^6$ systems that are the focus of this paper will contain effectively linear Fe−N−O groups.

Only a very few $\{FeNO\}^6$ heme complexes have been synthesized and characterized to date. The small number of

* To whom correspondence should be addressed.

(1) (a) Ribeiro, J. M. C.; Hazzard, J. M. H.; Nussenzveig, R. H.; Champagne, D. E.; Walker, F. A. *Science* **1993**, *260*, 539. (b) Anderson, J. F.; Champagne, D. E.; Weichsel, A.; Ribeiro, J. M. C.; Balfour, C. A.; Dress, V.; Montfort, W. R. *Biochemistry* **1997**, *36*, 4423.

(2) Valenzuela, J. G.; Walker, F. A.; Ribeiro, J. M. C. *J. Exp. Biol.* **1995**, *198*, 1519.

(3) Averill, B. A. *Chem. Rev.* **1996**, *96*, 2951 and references therein.

(4) Williams, P. A.; Fülöp, V.; Garman, E. F.; Saunders, N. F. W.; Ferguson, S. J.; Hajdu, J. *Nature* **1997**, *389*, 406.

(5) Obayashi, E.; Tsukamoto, K.; Adachi, S.; Takahashi, S.; Nomura, M.; Iizuka, T.; Shoun, H.; Shiro, Y. *J. Am. Chem. Soc.* **1997**, *119*, 7807.

(6) Wang, Y.; Averill, B. A. *J. Am. Chem. Soc.* **1996**, *118*, 3972.

(7) Fülöp, V.; Moir, J. W. B.; Ferguson, S. J.; Hajdu, J. *Cell* **1995**, *81*, 369.

(8) Enemark, J. H.; Feltham, R. D. *Coord. Chem. Rev.* **1974**, *13*, 339.

(9) Westcott, B. L.; Enemark; J. H. In *Inorganic Electronic Structure and Spectroscopy*; Lever, A. B. P., Solomon, E. I., Eds.; in press.

10.1021/ja984308q CCC: $18.00
Published on Web 05/20/1999

known species stems from the fact that these complexes have limited stability owing to the easy loss of the NO ligand and undergo reductive nitrosylation processes that lead to reduced iron species. Moreover, the iron nitrosyls are involved in complex equilibria with other nitrogen oxide species in the presence of the necessary excess NO. Although there have been solution spectroscopic, results[10] reported for {FeNO}^{6} porphyrins, there are substantial differences in reported spectroscopic parameters. The few structurally characterized examples include the five-coordinate species $[Fe(OEP)(NO)]^+$ [11] and the six-coordinate species $[Fe(TPP)(NO)(H_2O)]^+$ [11] and $[Fe(TPP)(HO\text{-}i\text{-}C_5H_{11})(NO)]^+$.[12]

However, there have been no previous reports of isolated, six-coordinate {FeNO}^{6} species with neutral nitrogen donors. We report the detailed syntheses and molecular structures of {FeNO}^{6} porphyrin complexes with several different neutral nitrogen axial ligands encompassing a range of basicities. The several molecular structures show that, unlike the {FeNO}^{7} systems, the trans sixth ligand distance is normal and the nitrosyl ligand does not impose a significant structural trans effect. More fundamentally, the structures demonstrate that these elusive species *can* be isolated as solids when appropriate care is taken. Finally, the infrared and UV−vis spectroscopic characterization reported herein provide important generalizations that allow for the differentiation of five- and six-coordinate species and the two common oxidation states of nitrosyliron porphyrins.

Experimental Section

General Information. All manipulations involving the addition of NO were carried out in an oxygen- and water-free environment using a double manifold vacuum line, Schlenkware, and cannula techniques. Chloroform was washed with sulfuric acid then water to remove the ethanol stabilizer. Chloroform and methylene chloride were distilled over CaH_2. Chlorobenzene was distilled over P_2O_5. Hexanes were distilled over sodium benzophenone. NO gas was purified by passing it through 4 Å molecular sieves immersed in a dry ice/ethanol slush bath to remove higher oxides of nitrogen.[13] All other chemicals were used as received from Aldrich or Fisher. IR spectra were recorded on a Perkin-Elmer 883 IR spectrophotometer as Nujol mulls; electronic spectra were recorded on a Perkin-Elmer Lambda 19 UV/vis/near-IR spectrometer. Representative electronic spectra cannot be obtained by simply dissolving the isolated {FeNO}^{6} compounds in an appropriate solvent. Therefore, electronic spectra for all of the {FeNO}^{6} compounds were obtained by preparing the compounds in situ in CH_2Cl_2 under an atmosphere of NO in a specially designed anaerobic cell with adjoining 1- and 10-mm cuvettes. The free base H_2OEP[14] was purchased from Midcentury Chemicals. The chloro- and (perchlorato)iron(III) derivatives were synthesized by modified literature methods.[15,16] *Caution!* Although we have experienced no problem with the procedures described in dealing with systems containing the perchlorate ion, they can detonate spontaneously and should be handled only in small quantities; in no case should such a system be heated above 30 °C, and other safety precautions are also warranted.[17]

Preparation of [Fe(OEP)(L)(NO)]ClO_4. The successful obtainment of crystalline solids of any particular six-coordinate nitrosyl−ligand complex is critically dependent on the choice of solvent and ligand concentration. The general procedure uses carefully purified solvent added to solid $[Fe(OEP)OClO_3]$ and solid or a dilute solution of the nitrogen-donating ligand (L) in an 8 × 150 mm glass tube inside an extralong Schlenk tube. NO gas was bubbled into the solution for several minutes. A dramatic color change occurred yielding a purple/pink solution. X-ray quality crystals were obtained by layering NO-saturated hexanes over the solution in the tubes. An NO atmosphere *must* be maintained inside the Schlenk tube during crystallization. These compounds immediately lose NO in solution if an NO atmosphere is not present.

Described below are the detailed procedures for obtaining X-ray quality single crystals of several different $[Fe(OEP)(L)(NO)]^+$ derivatives. Deviations from these specific conditions can result in the isolation of compounds other than the desired $[Fe(OEP)(L)(NO)]ClO_4$. Care must also be taken to avoid reductive nitrosylation. Several microcrystalline solids were also obtained by vapor diffusion of nonsolvent into a solution of $[Fe(OEP)OClO_3]$ and nitrogen-donating ligand (L) under an NO atmosphere.

[Fe(OEP)(1-MeIm)(NO)]ClO_4. To 15 mg (0.021 mmol) of $[Fe(OEP)OClO_3]$ and 20 μL of a 10% solution of 1-MeHIm in CH_2Cl_2 (0.025 mmol) was added 0.5 mL of C_6H_5Cl and 0.2 mL of CH_2Cl_2. IR (Nujol) ν(NO) = 1921 cm^{-1}. UV−vis (CH_2Cl_2): 410, 525, 558 nm.

[Fe(OEP)(Pz)(NO)]ClO_4·0.5C_6H_5Cl (1). To 13 mg (0.018 mmol) of $[Fe(OEP)OClO_3]$ and 2.4 mg (0.035 mmol) of pyrazole was added 0.7 mL of C_6H_5Cl and 0.3 mL of CH_2Cl_2. IR (Nujol) ν(NO) = 1894 cm^{-1}. UV−vis (CH_2Cl_2) 409, 524, 557 nm.

[Fe(OEP)(Iz)(NO)]ClO_4. To 17 mg (0.024 mmol) of $[Fe(OEP)OClO_3]$ and 28 mg (0.24 mmol) of indazole (benzopyrazole) was added 1 mL of CH_2Cl_2 or $CHCl_3$. IR (Nujol) ν(NO) = 1914 cm^{-1}. UV−vis (CH_2Cl_2) 408, 524, 556 nm.

{**[Fe(OEP)(NO)]$_2$Prz**}**(ClO_4)$_2$·1.8C_6H_5Cl.** To 12 mg (0.017 mmol) of $[Fe(OEP)OClO_3]$ and 7 mg (0.087 mmol) of pyrazine was added 0.7 mL of C_6H_5Cl and 0.3 mL of CH_2Cl_2. IR (Nujol) ν(NO) = 1899 cm^{-1}. UV−vis (CH_2Cl_2) 408, 524, 557 nm.

[Fe(OEP)(Prz)(NO)]ClO_4. To 13 mg (0.018 mmol) of $[Fe(OEP)OClO_3]$ and 15 mg (0.19 mmol) of pyrazine was added 0.7 mL of C_6H_5Cl and 0.3 mL of CH_2Cl_2. IR (Nujol) ν(NO) = 1911 cm^{-1}. UV−vis (CH_2Cl_2) 408, 524, 557 nm.

[Fe(OEP)(Pz)(NO)]ClO_4 (2). To 14 mg (0.020 mmol) of $[Fe(OEP)OClO_3]$ and 2.4 mg (0.035 mmol) of pyrazole was added 0.75 mL of CH_2Cl_2. IR (Nujol) ν(NO) = 1909 cm^{-1}. UV−vis (CH_2Cl_2) 409, 524, 557 nm.

X-ray Structure Determinations. All structure determinations were carried out on an Enraf-Nonius FAST area-detector diffractometer with a Mo rotating anode source ($\bar{\lambda}$ = 0.71073 Å). Our detailed methods and procedures for small molecule X-ray data collection with the FAST system have been described previously.[18] Data collections were performed at 130(2) K. The structures were solved using the direct methods program SHELXS-86;[19] subsequent difference Fourier syntheses led to the location of most of the remaining nonhydrogen atoms. The structures were refined against F^2 with the program SHELXL-97,[20,21] in which all data collected were used including negative

(10) (a) Wayland, B. B.; Olson, L. W. *J. Am. Chem. Soc.* **1974**, *96*, 6037. (b) Olson, L. W.; Schaeper, D.; Lançon, D.; Kadish, K. M. *J. Am. Chem. Soc.* **1982**, *104*, 2042. (c) Lançon, D.; Kadish, K. M. *J. Am. Chem. Soc.* **1983**, *105*, 5610. (d) Fujita, E.; Fajer, J. *J. Am. Chem. Soc.* **1983**, *106*, 6743. (e) Yoshimura, T. *Inorg. Chim. Acta* **1984**, *83*, 17. (f) Settin, M. F.; Fanning, J. C. *Inorg. Chem.* **1988**, *27*, 1431. (g) Mu, X. H.; Kadish, K. M. *Inorg. Chem.* **1988**, *27*, 4720. (h) Hoshino, M.; Ozawa, K.; Seki, H.; Ford, P. C. *J. Am. Chem. Soc.* **1993**, *115*, 9568. (i) Ozawa, S.; Sakamoto, E.; Ichikawa, T.; Watanabe, Y.; Morishima, I. *Inorg. Chem.* **1995**, *34*, 6362.

(11) Scheidt, W. R.; Lee, Y. J.; Hatano, K. *J. Am. Chem. Soc.* **1984**, *106*, 3191.

(12) Yi, G.-B.; Chen, L.; Khan, M. A.; Richter-Addo, G. B. *Inorg. Chem.* **1997**, *36*, 3876.

(13) Dodd, R. E.; Robinson, P. L. *Experimental Inorganic Chemistry*; Elsevier: New York, 1957; pp 233−234.

(14) Abbreviations: OEP, dianion of octaethylporphyrin; TPP, dianion of tetraphenylporphyrin; TpivPP, dianion of picket fence porphyrin; protoIX, dianion of protoporphyrin IX; Porph, a generalized porphyrin dianion; Pz, pyrazole; Iz, indazole (benzopyrazole); Prz, pyrazine; 1-MeIm, 1-methylimidazole; 4-CNPy, 4-cyanopyridine; 2-MePrz, 2-methylpyrazine; PMS, pentamethylene sulfide; 1,2-Me_2Im, 1,2-dimethylimidazole; 2-MeHIm, 2-methylimidazole; 4-MeTHZ, 4-methylthiazole; Thx, 1,4-thioxane; 4-MePip, 4-methylpiperidine; Py, pyridine; 4-NMe_2Py, 4-(dimethylamino)pyridine; 3-ClPy, 3-chloropyridine; 1-VinIm, 1-vinylimidazole; 1-BzlIm, 1-benzylimidazole; Pip, piperidine; Np, porphyrinato nitrogen.

(15) (a) Adler, A. D.; Longo, F. R.; Kampus, F.; Kim, J. *J. Inorg. Nucl. Chem.* **1970**, *32*, 2443. (b) Buchler, J. W. In *Porphyrins and Metalloporphyrins*; Smith, K. M., Ed.; Elsevier Scientific Publishing: Amsterdam, The Netherlands, 1975; Chapter 5.

(16) Dolphin, D. H.; Sams, J. R.; Tsin, T. B. *Inorg. Chem.* **1977**, *16*, 711.

(17) Wolsey, W. C. *J. Chem. Educ.* **1973**, *50*, A335; *Chem. Eng. News* **1983**, *61* (Dec. 5), 4; **1963**, *41* (July 8), 47.

(18) Scheidt, W. R.; Turowska-Tyrk, I. *Inorg. Chem.* **1994**, *33*, 1314.

(19) Sheldrick, G. M. *Acta Crystallogr.* **1990**, *A46*, 467.

(20) Sheldrick, G. M. *J. Appl. Cryst.*, manuscript in preparation.

Table 1. Crystallographic Details for [Fe(OEP)(L)(NO)]ClO_4 Derivatives at 130(2) K[a]

L	1-MeIm	Pz(**1**)	Iz	Prz/2	Prz	Pz(**2**)
formula	$[Fe(N_4C_{36}H_{44})(C_4H_6N_2)(NO)]ClO_4$	$[Fe(N_4C_{36}H_{44})(C_3H_4N_2)(NO)]ClO_4 \cdot 0.5C_6H_5C1$	$[Fe(N_4C_{36}H_{44})(C_7H_6N_2)(NO)]ClO_4$	$\{[Fe(N_4C_{36}H_{44})(NO)]_2(C_4H_4N_2)](ClO_4)_2\} \cdot 1.8C_6H_5Cl$	$[Fe(N_4C_{36}H_{44})(C_4H_4N_2)(NO)]ClO_4$	$[Fe(N_4C_{36}H_{44})(C_3H_4N_2)(NO)]ClO_4$
fw	800.17	842.42	836.20	1718.81	804.55	801.46
a, Å	9.3223(5)	10.5062(5)	10.1175(4)	12.748(2)	10.4276(12)	10.4526(2)
b, Å	19.1403(9)	13.705(3)	13.1764(9)	22.8417(16)	10.597(2)	10.6607(10)
c, Å	21.5806(12)	14.5932(14)	29.975(3)	14.8903(10)	18.353(2)	18.2497(16)
α, deg		80.136(7)			83.267(16)	82.315(5)
β, deg	98.795(3)	82.344(7)	96.430(5)	99.677(5)	81.528(7)	81.176(8)
γ, deg		77.504(10)			76.541(10)	75.624(5)
V, Å^3	3805.4(3)	2011.0(5)	3970.9(5)	4274.0(9)	1943.6(5)	1936.9(3)
Z	4	2	4	2	2	2
space group	$P2_1/n$	$P\bar{1}$	$P2_1/n$	$P2_1/c$	$P\bar{1}$	$P\bar{1}$
D_c, g/cm^3	1.397	1.391	1.399	1.336	1.375	1.384
F(000)	1688	886	1760	1805	846	842
μ, mm^{-1}	0.521	0.529	0.503	0.523	0.511	0.514
total data colld	27119	14912	23740	26189	18726	18233
unique data	9275 ($R_{int} = 0.0676$)	8826 ($R_{int} = 0.1003$)	8813 ($R_{int} = 0.0852$)	9146 ($R_{int} = 0.0676$)	9960 ($R_{int} = 0.0588$)	9749 ($R_{int} = 0.0676$)
final *R* indices[b] [I > 2σ(I)]	$R_1 = 0.0504$, $wR_2 = 0.1126$	$R_1 = 0.0693$, $wR_2 = 0.1922$	$R_1 = 0.0806$, $wR_2 = 0.1943$	$R_1 = 0.0655$, $wR_2 = 0.1607$	$R_1 = 0.1056$, $wR_2 = 0.2584$	$R_1 = 0.1026$, $wR_2 = 0.2736$
final *R* indices [for all data]	$R_1 = 0.0614$, $wR_2 = 0.1192$	$R_1 = 0.0828$, $wR_2 = 0.2048$	$R_1 = 0.0912$, $wR_2 = 0.2020$	$R1 = 0.0848$, $wR_2 = 0.1761$	$R_1 = 0.1717$, $wR_2 = 0.3065$	$R_1 = 0.1310$, $wR_2 = 0.3049$

[a] All data collected with Mo Kα radiation; $\bar{\lambda} = 0.71073$ Å. [b] Refinement method on F^2 (SHELXL-97).

intensities. Hydrogen atoms of the porphyrin ligand and the solvent molecules were idealized with the standard SHELXL-97 idealization methods. A modified[22] version of the absorption correction program DIFABS was applied to some of the structures. Brief crystal data are listed in Table 1. Complete crystallographic details for all of the structures are included in the Supporting Information. Some type of minor crystallographic disorder was found in all of the structure determinations and are detailed below.

[Fe(OEP)(1-MeIm)(NO)]ClO_4. One ethyl group is disordered over two positions (up and down) with respect to the porphyrin plane.

[Fe(OEP)(Pz)(NO)]$ClO_4 \cdot 0.5C_6H_5Cl$ (1). One-half of a molecule of chlorobenzene per asymmetric unit is disordered around an inversion center. A rigid-group refinement was used to define some of the "missing" atoms. This rigid-group constraint was used in the early stages and was released near the end of the refinement.

[Fe(OEP)(Iz)(NO)]ClO_4. Two ethyl groups are disordered (up and down) with respect to the porphyrin plane. Two oxygen atoms of the perchlorate anion also have two positions.

{[Fe(OEP)(NO)]$_2$Prz}$(ClO_4)_2 \cdot 1.8C_6H_5Cl$. There is a partially occupied molecule of chlorobenzene in the asymmetric unit. In addition, there is up/down disorder in one ethyl group and its *β* carbon with refined occupancies near 50%.

[Fe(OEP)(Prz)(NO)]ClO_4. There is a partially occupied solvent molecule disordered around an inversion center and three oxygen atoms of the perchlorate anion have two positions.

[Fe(OEP)(Pz)(NO)]ClO_4 (2). This crystalline form is isomorphous with [Fe(OEP)(Prz)(NO)]ClO_4. One ethyl group and its *β* carbon are disordered over two positions. The solvent molecule has a greater occupancy in this isomorph, and the perchlorate anion is now ordered. The nitrogen atom of the nitrosyl ligand in both isomorphs has a large temperature factor along the Fe−N−O bond direction and an unusually short Fe−N(NO) bond length was seen in both isomorphs.

Results

Several [Fe(OEP)(L)(NO)]$^+$ species (L = neutral nitrogen donor) have been synthesized under carefully controlled, empirically determined conditions. Isolated crystalline solids were obtained with the axial ligands summarized in Chart 1. X-ray structures were obtained for six crystalline species with four of the ligands shown in Chart 1 (L = 1-MeIm, Pz, Iz, Prz). The use of the exo-bidentate ligand pyrazine yielded a binuclear species ({[Fe(OEP)(NO)]$_2$Prz}$(ClO_4)_2$) where the pyrazine bridges two iron porphyrins as well as a mononuclear species ([Fe(OEP)(Prz)(NO)]ClO_4) with one pyrazine ligand bound per iron porphyrin. Two crystalline forms were obtained with the ligand pyrazole (denoted as [Fe(OEP)(Pz)(NO)]ClO_4(**1**) and [Fe(OEP)(Pz)(NO)]ClO_4(**2**)). They differ in unit cell solvent content and each complex has a distinctly different environment around the nitrosyl ligand. Brief crystallographic details for these six structures are given in Table 1. Structures of [Fe(OEP)(1-MeIm)(NO)]ClO_4, [Fe(OEP)(Pz)(NO)]ClO_4(**1**), [Fe(OEP)(Iz)(NO)]ClO_4, and {[Fe(OEP)(NO)]$_2$Prz}$(ClO_4)_2$ will be described in some detail while details of the structures of [Fe(OEP)(Prz)(NO)]ClO_4 and [Fe(OEP)(Pz)(NO)]ClO_4(**2**) can be found in the Supporting Information. Selected bond parameters for the first four derivatives are given in Table 2. Although the identity of the ligands is clear in the last two structures, the metrical usefulness of the bond parameters is limited. The structures are

Chart 1. Axial Ligands Used in This Study

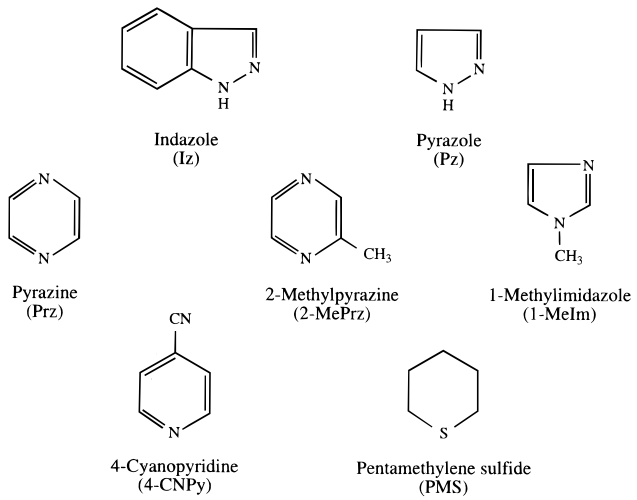

(21) $R_1 = \sum||F_o| - |F_c||/\sum|F_o|$ and $wR_2 = \{\sum[w(F_o^2 - F_c^2)^2]/\sum[wF_o^4]\}^{1/2}$. The conventional *R*-factors R_1 are based on *F*, with *F* set to zero for negative F^2. The criterion of $F^2 > 2\sigma(F^2)$ was used only for calculating R_1. *R*-factors based on F^2 (wR_2) are statistically about twice as large as those based on *F*, and *R*-factors based on ALL data will be even larger.

(22) The process is based on an adaptation of the DIFABS[23] logic to area detector geometry by Karaulov: Karaulov, A. I.; School of Chemistry and Applied Chemistry, University of Wales, College of Cardiff, Cardiff CF1 3TB, UK, personal communication.

Table 2. Summary of Coordination Group Geometry for {FeNO}^{6} Complexes and Complexes for Comparison

complex	Fe−N_p[a]	Fe−N_{NO}[a]	∠FeNO[b]	Fe−L[a]	N−O[a]	Δ[a]	ref
A. {FeNO}^{6} Metalloporphyrin Derivatives							
[Fe(OEP)(1-MeIm)(NO)]$^+$	2.003(5)	1.6465(17)	177.28(17)	1.9889(16)	1.135(2)	0.02[c]	this work
[Fe(OEP)(Pz)(NO)]$^+$ (**1**)	2.004(5)	1.627(2)	176.9(3)	1.988(2)	1.141(3)	0.01[c]	this work
[Fe(OEP)(Iz)(NO)]$^+$	1.996(4)	1.632(3)	177.6(3)	2.010(3)	1.136(4)	0.04[c]	this work
{[Fe(OEP)(NO)]$_2$Prz}$^{2+}$	1.995(8)	1.632(3)	176.5(3)	2.039(2)	1.131(4)	0.06[c]	this work
[Fe(TPP)(H_2O)(NO)]$^+$	1.999(6)	1.652(5)	174.4(10)	2.001(5)	1.150	NA[d]	11
[Fe(TPP)(HO-*i*-C_5H_{11})(NO)]$^+$	2.013(3)	1.776(5)	177.1(7)	2.063(3)	0.925(6)	0.05[c,e]	12
[Fe(TpivPP)(NO_2)(NO)]	1.996(4)	1.671(2)	169.3(2)	1.998(2)	1.1443(3)	0.09[c]	24
[Fe(OEP)(NO)]$^+$	1.994(3)	1.644(3)	176.9(3)		1.112(4)	0.29[c]	11
B. {FeNO}^{7} Metalloporphyrin Derivatives							
[Fe(TPP)(NO)]	2.001(3)	1.717(7)	149.2(6)		1.122(12)	0.21[c]	25
[Fe(OEP)(NO)]	2.010(13)	1.7307(7)	142.74(8)		1.1677(11)	0.27[c]	26
[Fe(TPP)(NO)(l-MeIm)]	2.008(12)	1.743(4)	142.1(6)	2.180(4)	1.121(8)	0.07[c]	27
[Fe(TPP)(NO) (4-MePip)](**1**)	2.004(9)	1.721(10)	138.5(11)	2.328(10)	1.141(13)	0.09[c]	28
[Fe(TPP)(NO)(4-MePip)](**2**)	1.998(10)	1.740(7)	143.7(6)	2.463(7)	1.112(9)	0.11[c]	28
C. Other Metalloporphyrin Derivatives (Fe(III))							
[Fe(TPP)(1-MeIm)$_2$]$^+$	1.982(11)			1.974(6)		0.0[f]	29
[Fe(ProtoIX)(1-MeIm)$_2$]$^+$	1.991(16)			1.977(16)		0.03	30
[Fe(TMP)(1-MeIm)$_2$]$^+$	1.988(20)			1.970(7)		0.0[f]	31
[Fe(TPP)(Py)$_2$]$^+$	1.982(7)			2.003(3)		0.03	32
[Fe(TPP)(4-CNPy)$_2$]$^+$	1.952(7)			2.002(8)		0.05	33
[Fe(OEP)(4-NMe_2Py)$_2$]$^+$	2.002(4)			1.995(3)		0.0[f]	31
[Fe(OEP)(3-ClPy)$_2$]$^+$	1.995(6)			2.031(2)		0.0[f]	34
D. Other Metalloporphyrin Derivatives (Fe(II))							
[Fe(TPP)(1-VinIm)$_2$]	2.001(2)			2.004(2)		0.0[f]	35
[Fe(TPP)(1-BzlIm)$_2$]	1.993(9)			2.017(4)		0.0[f]	35
[Fe(TPP)(1-MeIm)$_2$]	1.997(6)			2.014(2)		0.0[f]	36
[Fe(TPP)(Pip)$_2$]	2.004(4)			2.127(3)		0.0[f]	37
[Fe(TPP)(Pz)$_2$]	1.987(8)			1.99(3)		0.03	38

[a] Value in Å. [b] Value in degrees. [c] Displacement of the metal atom out of the 24-atom porphyrin plane towards NO. [d] Obscured by required crystallographic disorder. [e] Displacement of the metal atom from the mean plane of the four nitrogen atoms. [f] Required to be zero by crystallographic symmetry.

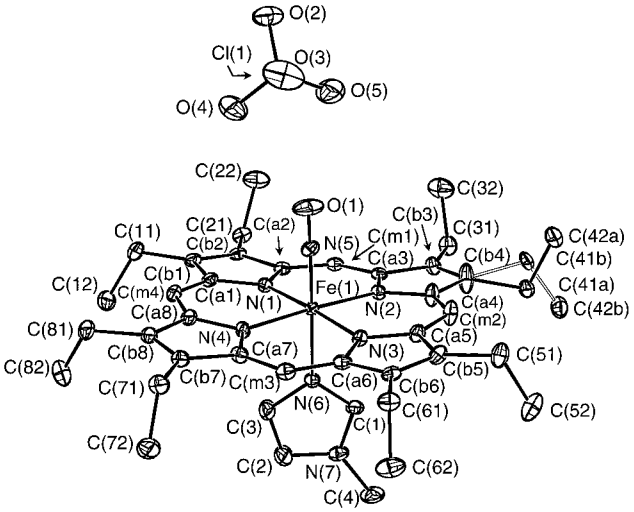

Figure 1. ORTEP diagram of [Fe(OEP)(1-MeIm)(NO)]ClO_4 illustrating the atomic labeling scheme and the disorder in the ethyl group; 50% probability ellipsoids are illustrated.

included, nevertheless, because they are a key part of understanding the trends of the NO vibrations in the IR spectra of these [Fe(OEP)(L)(NO)]$^+$ complexes (vide infra). Tables listing complete crystallographic details, atomic coordinates, bond distances and angles, anisotropic temperature factors, and fixed hydrogen atom positions are provided for all six structures in the Supporting Information.

ORTEP diagrams for [Fe(OEP)(1-MeIm)(NO)]ClO_4, [Fe(OEP)(Pz)(NO)]ClO_4 (**1**), [Fe(OEP)(Iz)(NO)]ClO_4, and {[Fe(OEP)(NO)]$_2$Prz}$(ClO_4)_2$ are given in Figures 1−4. The closest perchlorate anion is drawn in each case. In all of the structures the nitrosyl ligands are ordered and not required by symmetry

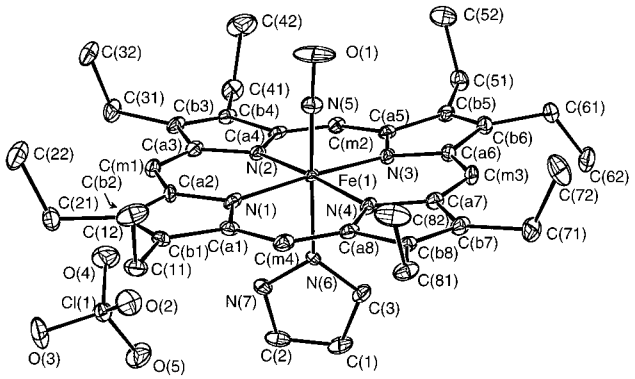

Figure 2. ORTEP diagram of [Fe(OEP)(Pz)(NO)]ClO_4 (**1**) displaying the labeling scheme and 50% probability ellipsoids.

to be linear. Several of the structures are plagued with the frequently occurring "up/down" disorder of an ethyl group as detailed in the Experimental Section. This type of disorder is found in [Fe(OEP)(1-MeIm)(NO)]ClO_4 (Figure 1); both orientations of the ethyl group are depicted with open and closed bonds. The ethyl group disorder, if present, is not depicted in the other ORTEP diagrams for sake of clarity. In the structure of {[Fe(OEP)(NO)]$_2$Prz}$(ClO_4)_2$, half of the "dimer" is unique, the other half being generated by an inversion center located at the center of the pyrazine ring. The labeling schemes displayed in these figures are those used in the corresponding diagrams and tables. Formal diagrams of the porphinato cores illustrating the averaged bond parameters for [Fe(OEP)(1-MeIm)(NO)]ClO_4, [Fe(OEP)(Pz)(NO)]ClO_4 (**1**), [Fe(OEP)(Iz)(NO)]ClO_4, and {[Fe(OEP)(NO)]$_2$Prz}$(ClO_4)_2$ are given in Figure 5. Figure 5 also displays the deviation of the atoms from the 24-atom mean plane; positive values, in units of 0.01 Å, are toward the nitrosyl ligand.

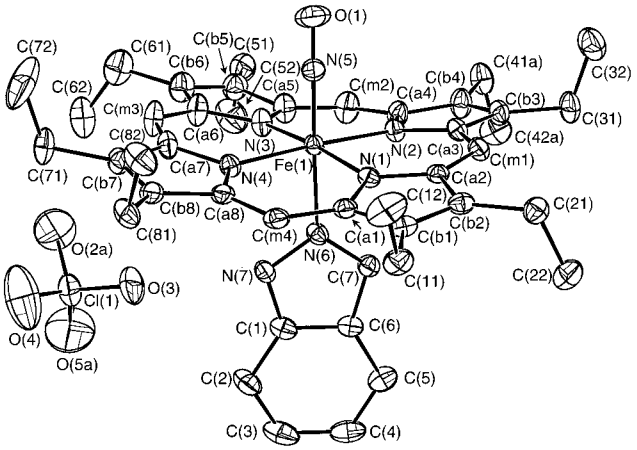

Figure 3. ORTEP diagram of [Fe(OEP)(Iz)(NO)]ClO_4. The combination of reverse doming and ruffling of the porphyrin core is best seen in this derivative; 50% probability ellipsoids are displayed.

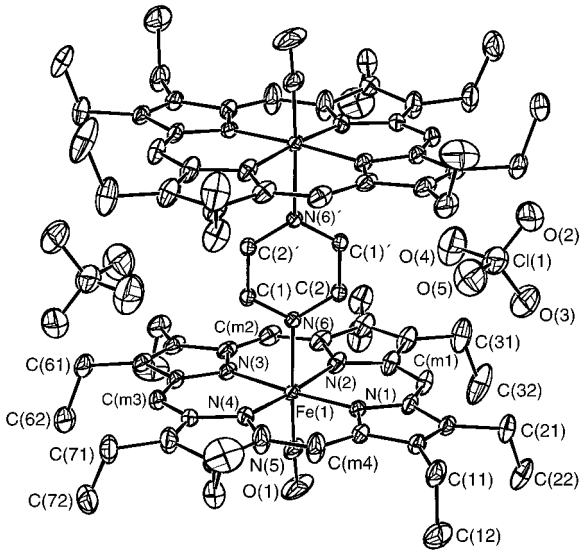

Figure 4. ORTEP diagram of the binuclear species {[Fe(OEP)(NO)]$_2$Prz}$(ClO_4)_2$. A crystallographic inversion center is located at the center of the bridging pyrazine ring; 50% probability ellipsoids are illustrated.

Similar diagrams for [Fe(OEP)(Prz)(NO)]ClO_4 and [Fe(OEP)(Pz)(NO)]ClO_4 (**2**) are provided in the Supporting Information (Figures S1 and S2).

The electronic spectrum of [Fe(OEP)(1-MeIm)(NO)]$^+$ in CH_2Cl_2 is shown in Figure 6. Also shown in Figure 6 are the spectra of the five-coordinate {FeNO}^{6} species, [Fe(OEP)(NO)]$^+$, the {FeNO}^{7} mixed-ligand six-coordinate species, [Fe(OEP)(1-MeIm)(NO)], and the five-coordinate {FeNO}^{7} species, [Fe(OEP)(NO)] in CH_2Cl_2 for subsequent discussion. Table 3 gives electronic spectral data for all {FeNO}^{6} mixed-ligand six-coordinate species synthesized in this study, as well as related species for comparison. Electronic spectra for all of the {FeNO}^{6} compounds were obtained by preparing the compounds in situ in CH_2Cl_2 under an atmosphere of NO in a specially designed anaerobic cell with adjoining 1- and 10-mm cuvettes.

The infrared spectrum of all of the nitrosyl species displays an intense NO band. Table 4 lists the solid-state NO stretching frequencies for all of the isolated {FeNO}^{6} mixed-ligand six-coordinate species. Also listed in the table are the NO frequencies for [Fe(OEP)(NO)]$^+$ and the two six-coordinate {FeNO}^{6} derivatives with neutral oxygen-donating axial ligands. Those derivatives for which structural details are provided in this paper

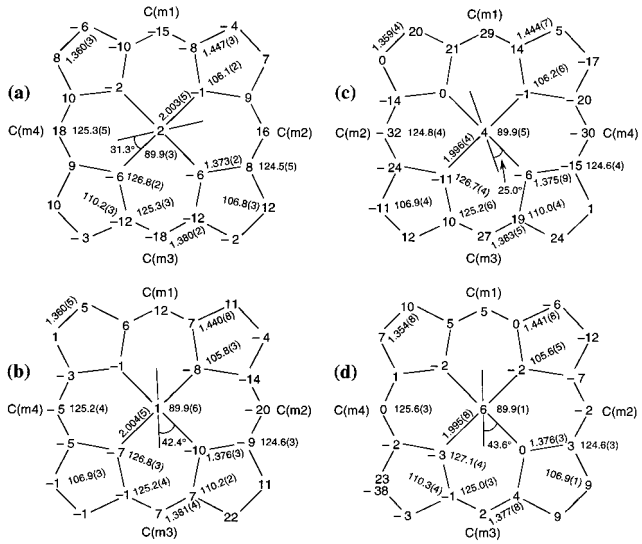

Figure 5. Formal diagrams of the porphinato cores of (a) [Fe(OEP)(1-MeIm)(NO)]ClO_4, (b) [Fe(OEP)(Pz)(NO)]ClO_4 (**1**), (c) [Fe(OEP)(Iz)(NO)]ClO_4, and (d) {[Fe(OEP)(NO)]$_2$Prz}$(ClO_4)_2$, illustrating the displacement of each unique atom from the mean plane of the 24-atom porphinato cores in units of 0.01 Å. Positive values are toward the nitrosyl ligand. The two entries for (Cb8) in (d) are the two positions of the carbon atom which is disordered above and below the plane. The averaged values of each type of bond distance and angle in the porphinato cores are given. Also displayed are the dihedral angles between the mean plane of the five- or six-membered ring of the axial ligand and the closest Np−Fe−N_L plane.

are noted. The stretching frequencies fall into two distinct classes as described in the Discussion.

Discussion

Syntheses. Several six-coordinate {FeNO}^{6} porphinato complexes with neutral, nitrogen-donating axial ligands (Chart 1) trans to the nitrosyl ligand have been synthesized and characterized. To our knowledge, no {FeNO}^{6} porphyrin complex with a neutral nitrogen-donating ligand trans to nitric oxide had been isolated prior to this study. Not only have we been able to isolate these species, we have also been able to obtain single crystals of many of the derivatives. The synthesis involves addition of excess NO to solutions of [Fe(OEP)($OClO_3$)] and experimentally determined quantities of the neutral nitrogen-donating ligand (L) under an inert atmosphere. The isolation of these complexes as solids has previously remained elusive due to several synthetic difficulties. One of the synthetic problems, apparently not always previously recognized, is the high lability of the nitrosyl ligand in {FeNO}^{6} porphyrin complexes. This condition requires that all attempts to synthesize and crystallize these {FeNO}^{6} complexes must be carried out under an NO atmosphere. This requirement has prompted the development of special crystallization techniques. The reactions and crystallizations are done in small diameter (8 mm) glass tubes inside a Schlenk tube. Hexanes are saturated with NO outside of the reaction tubes (inside the Schlenk tube) and then are layered over the reaction mixture via syringe; the NO atmosphere is maintained in the Schlenk tube throughout the crystallization experiment.

The lability of the NO ligand also means that NO can be easily replaced by the neutral-nitrogen donors to yield bis-ligated iron(III) complexes even in the presence of an atmosphere of NO. Therefore, in some cases a limited amount of the nitrogen ligand should be present. This condition applies particularly to

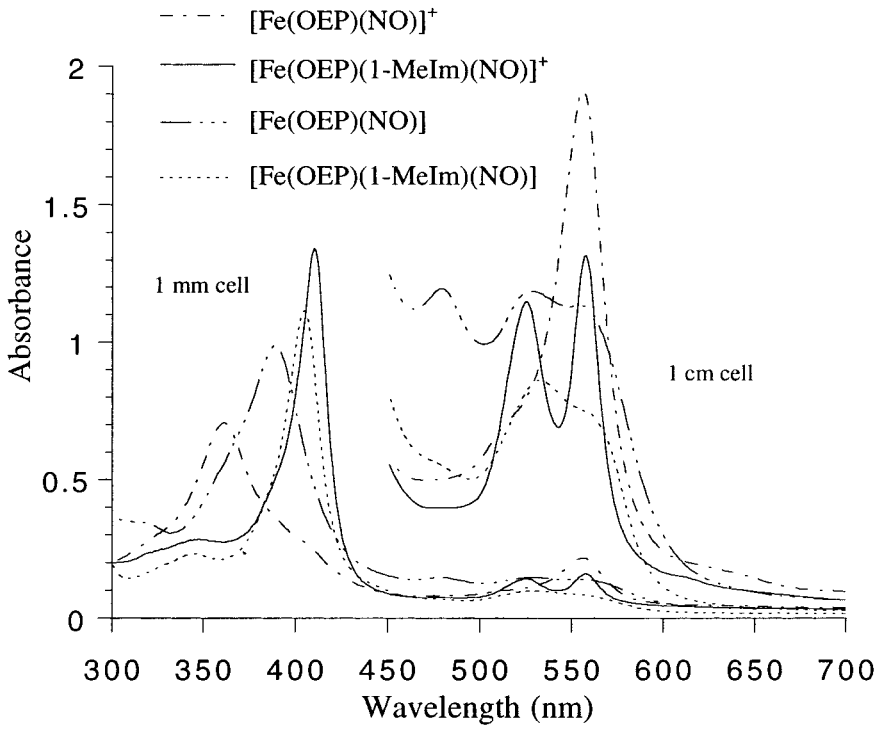

Figure 6. UV−vis spectrum of [Fe(OEP)(1-MeIm)(NO)]$^+$ (—). For comparison, the spectra for five-coordinate [Fe(OEP)(NO)]$^+$ (-·-·-·), five-coordinate [Fe(OEP)(NO)] (-···) and six-coordinate [Fe(OEP)(1-MeIm)(NO)] (····) are also displayed. All porphyrin complexes are in CH_2Cl_2 solution at approximately equal concentrations.

Table 3. Electronic Spectral Data for Selected Porphyrin Complexes in CH_2Cl_2

complex	λ_{max} (nm)		
[Fe(OEP)(L)(NO)]$^+$			
[Fe(OEP)(1-MeIm)(NO)]$^+$	410	525	558
[Fe(OEP)(1,2-Me$_2$Im) (NO)]$^+$	412	528	560
[Fe(OEP)(2-MeHIm)(NO)]$^+$	413	528	560
[Fe(OEP)(Iz)(NO)]$^+$	408	524	556
[Fe(OEP)(Pz)(NO)]$^+$	409	524	557
[Fe(OEP)(Prz)(NO)]$^+$	408	524	557
[Fe(OEP)(2-MePrz)(NO)]$^+$	408	524	557
[Fe(OEP)(4-CNPy)(NO)]$^+$	408	524	557
[Fe(OEP)(PMS)(NO)]$^+$	416	528	560
[Fe(OEP)(4-MeTHZ)(NO)]$^+$	413	527	560
[Fe(OEP)(Thx)(NO)]$^+$	415	528	559
Five, Six-Coordinate Iron(III)			
[Fe(OEP)(NO)]$^+$	359	515(sh)	557
[Fe(OEP)(1-MeIm)$_2$]$^+$	403	525	554
[Fe(OEP)(NO$_2$)(NO)]	415	528	560
Five, Six-Coordinate {FeNO}^{7}			
[Fe(OEP)(NO)]	389 479	529	554
[Fe(OEP)(1-MeIm)(NO)]	405	533	562(sh)

Table 4. Solid-State Nitrosyl Stretching Frequencies for Several {FeNO}^{6} Porphyrin Complexes[a]

complex	ν(NO) (cm^{-1})	ref
[Fe(OEP)(1-MeIm)(NO)]$^+$	1921[b,c]	this work
[Fe(OEP)(4-CNPy)(NO)]$^+$	1916	this work
[Fe(OEP)(Iz)(NO)]$^+$	1914[b]	this work
[Fe(OEP)(PMS)(NO)]$^+$	1913	this work
[Fe(OEP)(2-MePrz)(NO)]$^+$	1912	this work
[Fe(OEP)(Prz)(NO)]$^+$	1911[b]	this work
[Fe(OEP)(Pz)(NO)]$^+$(**2**)	1909[b,d]	this work
{[Fe(OEP)(NO)]$_2$Prz}$^{2+}$	1899[b]	this work
[Fe(OEP)(Pz)(NO)]$^+$(**1**)	1894[b,d]	this work
[Fe(OEP)(1-MeIm)(NO)]$^+$	1890[c]	this work
[Fe(OEP)(NO)]$^+$	1862[e]	11
[Fe(TPP)(H$_2$O)(NO)]$^+$	1937[e]	11
[Fe(TPP)(HO-*i*-C$_5$H$_{11}$)(NO)]$^+$	1935[e]	12

[a] Nujol mull. [b] Structure determination presented. [c,d] Two crystalline modifications. [e] KBr pellet.

the ligands 1-methylimidazole and pyrazole. This necessity to limit the amount of ligand is in direct contrast to the need to use large excesses of the same ligands to get the mixed-ligand {FeNO}^{7} species. It is thus clear that the ligand affinities of ligands trans to the nitrosyl, for the two oxidation states of iron, are much different. In some cases a modest excess of base is necessary to ensure formation of the mixed-ligand {FeNO}^{6} complex. This is necessary for the ligands indazole, 2-methylpyrazine, 4-cyanopyridine and pentamethylene sulfide. A guess for the initial ligand concentrations can be made (based on the pK_as) but usually the appropriate amount must then be refined experimentally. In the case of the exo-bidentate ligand pyrazine, adding a limited amount of ligand promotes the formation of the species which has one ligand bridging two {FeNO}^{6} porphyrins. In addition, we have observed that the choice of solvent can either lead to different polymorphs of the same species or more frequently, to unsatisfactory crystals and powders. Several different methods and conditions were used for each ligand in our attempts to obtain X-ray quality crystals. Thus, careful attention to synthetic details, as described in the Experimental Section, is necessary to isolate the desired complex.

Another synthetic difficulty is the ease of reducing {FeNO}^{6} to {FeNO}^{7} porphyrin complexes under conditions of excess NO (reductive nitrosylation). This reduction process is aided by the presence of NO$^+$ acceptors (H_2O, ROH, and possibly an excess of some nitrogenous bases); care must be taken to eliminate these from the reaction system.

Molecular Structures. The structures of six [Fe(OEP)(L)(NO)]$^+$ complexes where L = 1-MeIm, Pz, Iz, Prz/2, and Prz have been determined. The X-ray structure determinations unambiguously confirm the ligation pattern of these new [Fe(OEP)(L)(NO)]$^+$ complexes. Geometric information about the

Fe−N−O group upon addition of the trans ligand can thus be obtained and compared to that of six-coordinate {FeNO}^{7} and five-coordinate {FeNO}^{6} complexes. The molecular structures of [Fe(OEP)(1-MeIm)(NO)]ClO_4, [Fe(OEP)(Pz)(NO)]ClO_4 (**1**), [Fe(OEP)(Iz)(NO)]ClO_4, and {[Fe(OEP)(NO)]$_2$Prz}$(ClO_4)_2$ are shown in Figures 1−4. The linearity of the Fe−N−O groups is evident; the Fe−N−O angles range from 176.5(3) to 177.6(3)° (Table 2). The linearity of the Fe−N−O group in these {FeNO}^{6} species is as expected,[8] and the values agree with the Fe−N−O angle (176.9(3)°) observed for the five-coordinate species [Fe(OEP)(NO)]$^+$.[11]

The Fe−N_{NO} bond lengths in these six-coordinate derivatives are very short and range from 1.627(2) to 1.6465(17) Å. These Fe−N_{NO} bond lengths are as short as or shorter than the Fe−N_{NO} bond (1.644(3) Å) seen for the five-coordinate species [Fe(OEP)(NO)]$^+$.[11] Thus, the addition of a sixth ligand does not affect the Fe−N−O bond angle or the Fe−N distance of the Fe−N−O group significantly from that seen in the five-coordinate {FeNO}^{6} species. However, the addition of the sixth ligand does strongly affect the position of the iron atom with respect to the porphyrin plane. In the five-coordinate derivative ([Fe(OEP)(NO)]$^+$), the iron atom is displaced by 0.29 Å out of the porphyrin plane towards the nitrosyl ligand. In the six-coordinate derivatives ([Fe(OEP)(L)(NO)]$^+$), the presence of the sixth (neutral nitrogen) ligand leads to the iron atom being nearly in the plane of the porphyrin core. Finally, the Fe−N(NO) bond distances of the {FeNO}^{6} species are quite distinctly shorter than the values seen in the {FeNO}^{7} species. The Fe−N_{NO} distance in the five- and six-coordinate {FeNO}^{7} are longer at 1.717(7)−1.743(4) Å (Table 2) and must reflect the substantial difference in π bonding between the linearly coordinated NO (in {FeNO}^{6} derivatives) and the partially bent Fe−N−O group of the {FeNO}^{7} species.

The substantial shortening of the Fe−N_{NO} bond lengths in the {FeNO}^{6} derivatives compared to the {FeNO}^{7} derivatives appear to be in conflict with the ready dissociation of the nitrosyl ligand in the {FeNO}^{6} species. However, the bond lengths are a reflection of the ground states, while the dissociation equilibria reflect kinetic factors. The 1.627(2) to 1.6465(17) Å Fe−N_{NO} bond distances observed in the {FeNO}^{6} species reflect the strong π bonding of two Fe−N π bonds and the concomitant linear Fe−N−O group. The longer Fe−N_{NO} bond distances in the {FeNO}^{7} systems reflects the diminished π bonding associated with the bending of the Fe−NO group. Despite the shorter Fe−N_{NO} bond distances in the {FeNO}^{6} species, this species loses NO much more easily than the {FeNO}^{7} species. The disparity in dissociation of NO reflects differences in the transition states for loss of the axial nitrosyl ligand. The differences in ligand binding constants in the two oxidation states is largely due to differences in the values of the ligand dissociation rates, while the association rates for the two oxidation states are more nearly equivalent.[39] This is similar to the dichotomy between thermodynamic and kinetic effects that are well recognized in the trans effects seen in structures and ligand-substitution reactions.[40]

The quite small (0.01−0.06 Å) iron atom displacements in the [Fe(OEP)(L)(NO)]$^+$ derivatives (Table 2) are all towards the NO ligand. The very small iron displacements and the short Fe−N_{NO} bond distances leads to quite close contacts between the nitrosyl nitrogen atom and the porphyrin nitrogen atoms. The steric interactions between the nitrogens of the nitrosyl and the porphyrin cause modest distortions in the porphyrin core as can be seen in Figure 5. In all four structures there is a modest reverse core doming of 0.03 to 0.06 Å that slightly increases the $N_{NO}\cdots N_p$ distances. These short N···N separations range from 2.58 to 2.68 Å with an average value of 2.63 Å and would be slightly smaller without the reverse doming. The reverse doming of the core can also be seen in Figure 2.[41]

The reverse doming is superimposed on a second (more dominant) core deformation. Formal diagrams describing the quantitative displacement of atoms from the mean porphyrin plane are given Figures 5, S1, and S2.[42] Five of the structures ([Fe(OEP)(1-MeIm)(NO)]ClO_4, [Fe(OEP)(Pz)(NO)]ClO_4 (**1**), [Fe(OEP)(Iz)(NO)]ClO_4, [Fe(OEP)(Prz)(NO)]ClO_4, and [Fe(OEP)(Pz)(NO)]ClO_4 (**2**)) display small to moderate ruffling of the porphyrin core, while the sixth derivative {[Fe(OEP)(NO)]$_2$Prz}$(ClO_4)_2$ shows a modest saddling of the core. The magnitude of the core nonplanarity is such that there will be no significant effect on the equatorial Fe−N_p bond distances. In all of the structures, the average Fe−N_p bond length (range 1.995(8)−2.004(5) Å) is that typical for low-spin iron(III) porphyrins.[43] The N_{NO}−Fe−N_L angles range from 177.46(11) to 178.75(8) Å. The orientation of the axial ligands with respect to the porphyrin plane is depicted in Figure 5. The angles range from 25.0 to 43.6°. This angle is 25.2° in [Fe(TPP)(1-MeIm)-

(23) Walker, N. P.; Stuart, D. *Acta Crystallogr., Sect. A* **1983**, *A39*, 158.
(24) Ellison, M. K.; Schulz, C. E.; Scheidt, W. R. *Inorg. Chem.* **1999**, *38*, 100.
(25) Scheidt, W. R.; Frisse, M. E. *J. Am. Chem. Soc.* **1975**, *97*, 17.
(26) Ellison, M. K.; Scheidt, W. R. *J. Am. Chem. Soc.* **1997**, *119*, 7404.
(27) Piciulo, P. L.; Scheidt, W. R. *J. Am. Chem. Soc.* **1976**, *98*, 1913.
(28) Scheidt, W. R.; Brinegar, A. C.; Ferro, E. B.; Kirner, J. F. *J. Am. Chem. Soc.* **1977**, *99*, 7315.
(29) Higgins, T. B.; Safo, M. K.; Scheidt, W. R. *Inorg. Chim. Acta* **1990**, *178*, 261.
(30) Little, R. G.; Dymock, K. R.; Ibers, J. A. *J. Am. Chem. Soc.* **1975**, *97*, 4532.
(31) Safo, M. K.; Gupta, G. P.; Walker, F. A.; Scheidt, W. R. *J. Am. Chem. Soc.* **1991**, *113*, 5497.
(32) Inniss, D.; Soltis, S. M.; Strouse, C. E. *J. Am. Chem. Soc.* **1988**, *110*, 5644.
(33) Safo, M. K.; Walker, F. A.; Raitsimring, A. M; Walters, W. P.; Dolata, D. P.; Debrunner, P. G.; Scheidt, W. R. *J. Am. Chem. Soc.* **1994**, *116*, 7760.
(34) Scheidt, W. R.; Geiger, D. K.; Haller, K. J. *J. Am. Chem. Soc.* **1982**, *104*, 495.
(35) Safo, M. K.; Scheidt, W. R.; Gupta, G. P. *Inorg. Chem.* **1990**, *29*, 626.
(36) (a) Steffen, W. L.; Chun, H. K.; Hoard, J. L.; Reed, C. A. *Abstracts of Papers*, 175th National Meeting of the American Chemical Society, Anaheim, CA, March 13−17, 1978; American Chemical Society: Washington, DC, 1978; INOR 15. (b) Hoard, J. L., personal communication.
(37) Radonovich, L. J.; Bloom, A.; Hoard, J. L. *J. Am. Chem. Soc.* **1972**, *94*, 2073.
(38) Hiller, W.; Hanack, M.; Mezger, M. G. *Acta Crystallogr., Sect. C* **1987**, *C43*, 1264.
(39) See, for example, Table II of reference 10h and references cited therein.
(40) Atwood, J. D. *Inorganic and Organometallic Reaction Mechanisms*; Brooks/Cole Publishing Co.: Monterey, CA, 1985; pp 51−55.
(41) The major types of core deformations are illustrated in Figure S3. Doming of the porphyrinato core can also be described as a C_{4v} saucering of the four pyrrole rings such that the perpendicular displacements of the β-carbon atoms are more displaced from the mean 24-atom plane than the α-carbons or the nitrogen atoms. These displacements are in the direction away from the central metal and represent the usual case (see Figure S3). Reverse doming is a relatively infrequently occurring core conformation in which the pattern of displacements of the β-carbon atoms and the α-carbon or nitrogen atoms are reversed. Thus, in this case the N-atoms and α-carbons are displaced out of the 24-atom mean plane away from the metal, and the β-carbons are displaced towards the metal.
(42) The calculation of the displacements from the mean plane of the porphyrin cores are based on the coordinates for the 24 atoms of the porphyrin core. In the case of {[Fe(OEP)(NO)]$_2$Prz}$(ClO_4)_2$ there is one β-carbon atom (Cb8) which is disordered over two positions (above and below the plane) with nearly equivalent populations. For this case the mean plane was calculated by using both atom coordinates. However, the calculation based on only the 23 ordered atoms gave essentially the same results.
(43) Scheidt, W. R.; Reed, C. A. *Chem.. Rev.* **1981**, *81*, 543.

(NO)].[27] As tabulated by Scheidt and Lee,[44] the average dihedral angle for five-coordinate imidazole complexes is 10.4 (7.4)°. For six-coordinate imidazole derivatives the angle is 21.0 (12.1)°. For five- and six-coordinate pyridine complexes the angles are 22.0 (14.9) and 28.5 (14.3)°.

From Table 2 we can see that the Fe−N_L bond lengths (range 1.988(2)−2.039(2) Å) in the $[Fe(OEP)(L)(NO)]^+$ complexes are only slightly longer than the Fe−N_L bond lengths of the bis-ligated iron(III) derivatives. The average Fe−N_L bond length for the bis-imidazole derivatives listed in Table 2 is 1.974 Å. In $[Fe(OEP)(1\text{-}MeIm)(NO)]ClO_4$, the Fe−$N_L$ bond length is increased by only 0.015 Å from this average. In $\{[Fe(OEP)(NO)]_2Prz\}(ClO_4)_2$, the Fe−$N_L$ bond length is increased by only 0.03 Å from the average of the closely related bis-pyridine derivatives (Table 2) which have a Fe−N_L bond length of 2.008 Å. It is clear that the nitrosyl ligand does not exert a structural trans effect in these $\{FeNO\}^6$ systems. In the $\{FeNO\}^7$ case there is a substantial structural trans effect. In the complex $[Fe(TPP)(1\text{-}MeIm)(NO)]$[27] the Fe−$N_L$ bond length increases by 0.17 Å compared to the Fe−N_L bond length in $[Fe(TPP)(1\text{-}MeIm)_2]$;[36] the increase is even larger in the piperidine systems. The disparity in the structural trans effect is no doubt integral to the large difference in reactivity between $\{FeNO\}^7$ and $\{FeNO\}^6$ porphyrin complexes both in model complexes and in the biological systems.

Electronic and Vibrational Spectroscopy. Although there have been several previously reported spectroscopic studies of five- and six-coordinate $\{FeNO\}^6$ porphyrins,[10,11] the spectral similarities and differences that could be used to assign iron oxidation state and coordination number have not been systematically addressed. Furthermore, some of the reported spectra are known to be mixtures.[10g,11] We report herein the spectra of five- and six-coordinate $\{FeNO\}^6$ and $\{FeNO\}^7$ systems using the same porphyrin ligand to demonstrate the unique identifying features of each species. It is to be noted that there can be problems in obtaining representative spectra of $\{FeNO\}^6$ species that arise from the high lability of the nitrosyl ligand and reductive nitrosylation. We have found that an NO atmosphere must be present and carefully purified solvents must be used to reproducibly obtain spectra of the $\{FeNO\}^6$ complexes. As noted earlier, in some cases, carefully limited concentrations of the neutral nitrogen-donating ligand are necessary to prevent displacement of the nitrosyl ligand.

Figure 6 illustrates the distinctive UV−vis spectrum of $[Fe(OEP)(1\text{-}MeIm)(NO)]^+$ in CH_2Cl_2. Indeed, the wavelength maxima (listed in Table 3), band shapes, and relative intensities for all of the $[Fe(OEP)(L)(NO)]^+$ complexes are quite similar. The spectrum of six-coordinate $[Fe(OEP)(NO_2)(NO)]$ is also similar.[24] From Figure 6 and Table 3 we can see that the Soret band for the $[Fe(OEP)(L)(NO)]^+$ derivatives is always red-shifted relative to all of the other possible species including $[Fe(OEP)(1\text{-}MeIm)_2]^+$. The other notable feature in the spectra of $[Fe(OEP)(L)(NO)]^+$ derivatives is in the visible region, where there are always distinctively sharp α and β bands. The intensities of the α and β bands are approximately $^1/_{10}$ of that of the Soret band. The unique electronic spectrum of the mixed-ligand six-coordinate $\{FeNO\}^6$ species persists in solution as long as there is an NO atmosphere. In the absence of an NO atmosphere or if the concentration of added neutral nitrogen-donor ligand is too high, the spectrum of the bis-ligated species ($[Fe(OEP)(L)_2]^+$) is observed.

Figure 6 also gives representative UV−vis spectra for other iron nitrosyl derivatives. Five-coordinate $[Fe(OEP)(NO)]^+$ is seen to have a very blue-shifted Soret band and a strong single feature in the visible which is about one-third of the intensity of the Soret band. The addition of a ligand shifts the Soret band strongly to the red, another sharp peak appears in the visible, and the relative intensities of the visible bands decrease by a factor of ∼3. Thus the distinction between the five- and six-coordinate $\{FeNO\}^6$ species is clear. The-five-coordinate $\{FeNO\}^7$ species, [Fe(OEP)(NO)], has a quite broad Soret band and a characteristic 480-nm band in addition to the other bands in the visible. Addition of the sixth ligand to give [Fe(OEP)(1-MeIm)(NO)] leads to a distinct sharpening of the Soret band and the disappearance of the 480-nm band. All four classes of nitrosyl compounds have distinctly different electronic spectral patterns uniquely identifying the coordination number and oxidation state of any nitrosyl derivative. Previously reported spectroscopic data for $\{FeNO\}^6$ porphyrin model complexes, obtained with consideration of the lability of the nitrosyl ligand and reductive nitrosylation, agree with our data.[10a,b,e,i] More importantly, the patterns observed in our spectra agree well with iron(III) nitrosyl heme protein spectroscopic data.[1,2,5,10h,45] In addition, spectra of the isoelectronic species, [Fe(Porph)(L)(CO)], exhibit similar wavelength maxima but not quite as distinct bands in the visible region.[46]

Electronic spectra are also useful in distinguishing the nitrosyl complex $[Fe(OEP)(L)(NO)]^+$ from the undesired bis-ligated $[Fe(OEP)(L)_2]^+$ side product. As shown in Figure 7, these two species are readily distinguished by the differences in the visible region of the spectra, even though both are low-spin, six-coordinate iron(III) species. However, as is also shown in Figure 7, the spectral distinction between $[Fe(OEP)(1\text{-}MeIm)_2]^+$ and the $\{FeNO\}^7$ species, [Fe(OEP)(1-MeIm)(NO)] is quite small.

These nitrosyl porphinato complexes display an intense NO band in the infrared. Although the entire set of $\{FeNO\}^6$ porphyrin complexes would appear to be a closely related set of species, they do show a quite broad range of nitrosyl stretching frequencies. The range of ν(NO) values reported in the literature for $\{FeNO\}^6$ porphyrin complexes is from 1764 to 1937 cm^{-1}, a variation of almost 200 cm^{-1}.[10a,e−g,i,12,24,47] The issue of precisely what structural information can be derived from a knowledge of nitrosyl stretching frequencies in the $\{FeNO\}^6$ derivatives is an active issue in our laboratory. However, the observed NO stretching frequencies for the six-coordinate $[Fe(OEP)(L)(NO)]^+$ complexes (L = neutral nitrogen) reported herein fall into a narrow range (1890−1921 cm^{-1}, Table 4). Indeed, most of the six-coordinate derivatives have an NO stretch in the much narrower range of 1912 ± 4 cm^{-1}. An imidazole derivative has a ν(NO) slightly higher (1921 cm^{-1}); three derivatives have substantially reduced (by about 15 cm^{-1}) NO stretching frequencies from the "typical" values of the first seven (Table 4). It is to be noted that these last three derivatives also have the same nitrogen ligands (Prz, Pz, and 1-MeIm) as those of compounds in the first group. The fact that three ligand set pairs of the $[Fe(OEP)(L)(NO)]^+$ complexes display two markedly different solid-state NO stretching frequencies has led us to examine this further; we believe that the difference can be attributed to solid-state effects. Two of the three compounds with the lowered values have been structurally

(44) Scheidt, W. R.; Lee, Y. J. *Struct. Bonding (Berlin)* **1987**, *64*, 1-70.

(45) (a) Shiro, Y.; Fujii, M.; Iizuka, T.; Adachi, S.; Tsukamoto, K.; Nakahara, K.; Shoun, H. *J. Biol. Chem.* **1995**, *270*, 1617. (b) Yoshimura, T.; Fujii, S.; Kamada, H.; Yamaguchi, K.; Suzuki, S.; Shidara, S.; Takakuwa, S. *Biochim. Biophys. Acta* **1996**, *1292*, 39.

(46) (a) Stolzenberg, A. M.; Strauss, S. H.; Holm, R. H. *J. Am. Chem. Soc.* **1981**, *103*, 4763. (b) Rougee, M.; Brault, D. *Biochemistry* **1975**, *14*, 4100. (c) Wang, C.-M.; Brinigar, W. S. *Biochemistry* **1979**, *18*, 4960.

(47) Guilard, R.; Lagrange, G.; Tabard, A.; Lançon, D.; Kadish, K. M. *Inorg. Chem.* **1985**, *24*, 3649.

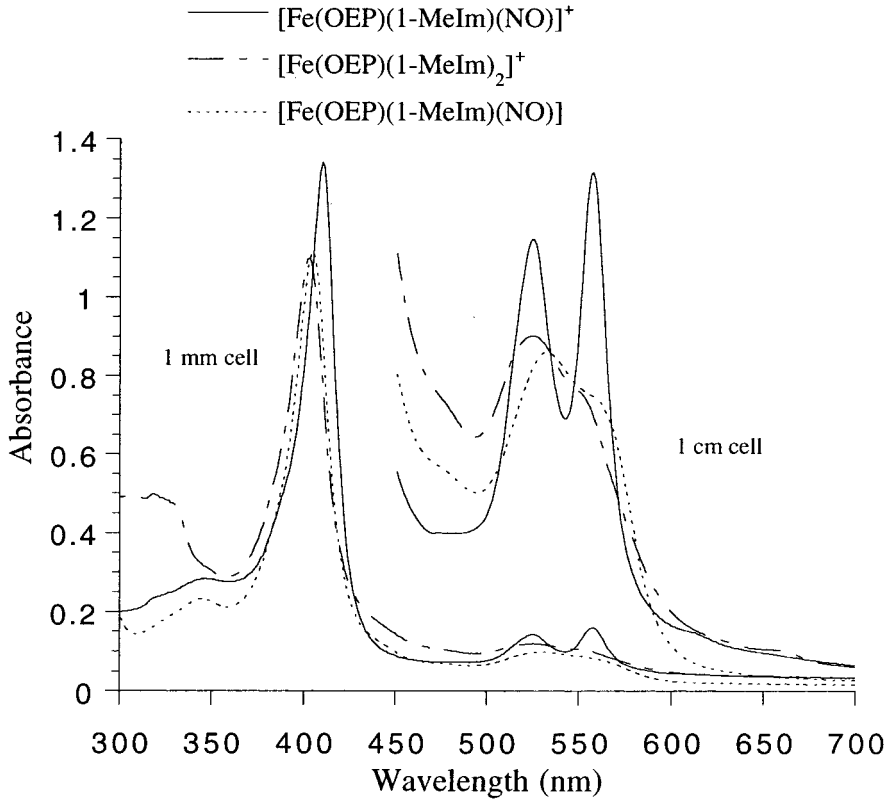

Figure 7. UV−vis spectra for $[Fe(OEP)(1\text{-}MeIm)(NO)]^+$ (—), $[Fe(OEP)(1\text{-}MeIm)_2]^+$ (— -), and [Fe(OEP)(1-MeIm)(NO)] (····). All porphyrin complexes are in CH_2Cl_2 solution at approximately equal concentrations.

characterized. The two pyrazole (Pz) complexes provide the clearest comparisons. In the derivative with the lowered ν(NO) ($[Fe(OEP)(Pz)(NO)]ClO_4$ (**1**)), the nitrosyl ligands from neighboring molecules closely approach each other in an unusual way. The two nitrosyl ligands shown in Figure 8 are related by an inversion center; the nitrosyl oxygen atoms are in near van der Waals contact with an O···O distance of 2.90 Å so as to form a weakly bound dimer. In the $[Fe(OEP)(Pz)(NO)]ClO_4$ (**2**) structure, the nitrosyl groups do not display any particular interaction and can be described as having well-separated nitrosyl units; a "feature" also displayed by all of the other nitrosyl derivatives with ν(NO) in the 1912 cm^{-1} region.[48] A similar close approach of nitrosyl ligand pairs is also in the structure of $\{[Fe(OEP)(NO)]_2Prz\}(ClO_4)_2$ as shown in Figure 9. In this complex, the O···O distance is 2.96 Å. In the related (monomeric) structure of $[Fe(OEP)(Prz)(NO)]ClO_4$, as in the remaining $[Fe(OEP)(L)(NO)]^+$ structures, there is again no recognizable nitrosyl−nitrosyl interaction. It is a reasonable presumption that a nitrosyl−nitrosyl interaction would also be found in the $[Fe(OEP)(1\text{-}MeIm)(NO)]^+$ structure with ν(NO) = 1890 cm^{-1}. Unfortunately, we have been unable to obtain crystals large enough for a structure analysis.

This dimeric (O···O) structural feature could affect ν(NO) either through an environmental effect, akin to changes in solution vibrational frequencies seen on changing solvents, or through a coupling of the two nitrosyl groups to yield symmetrically and antisymmetrically coupled vibrations. Only the antisymmetric stretch would be seen in the infrared, while the symmetric stretch would be seen in the Raman spectrum. We have attempted to measure the nitrosyl stretching frequencies in the resonance Raman spectra; unfortunately, any such features are very weak or unobserved under all of the conditions we have examined thus far. We are thus unable to distinguish which of these two possible mechanisms for ν(NO) variation is the probable explanation for the observed frequency shifts.

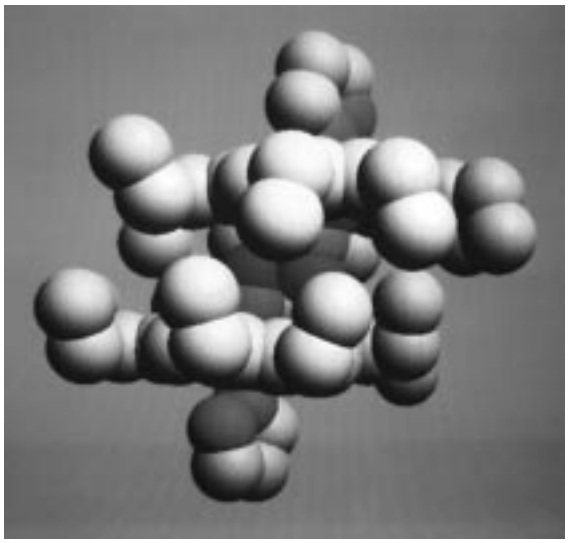

Figure 8. Space-filling diagram of the two closely interacting molecules of $[Fe(OEP)(Pz)(NO)]^+$ (**1**). The perchlorate anions, solvent molecules, and hydrogen atoms have been omitted for clarity. The two oxygen atoms of the nitrosyl ligands are related by an inversion center at the center of the diagram.

The nitrosyl stretching frequency of the $[Fe(OEP)(L)(NO)]^+$ derivatives are all found at *higher* frequency than that observed for five-coordinate $[Fe(OEP)(NO)]^+$.[11] This trend is the opposite of that seen for the $\{FeNO\}^7$ porphyrin complexes, where the six-coordinate derivatives are observed to have *lower* nitrosyl stretching frequencies than the related five-coordinate species.

(48) The entries $[Fe(OEP)(4\text{-}CNPy)(NO)]^+$ and $[Fe(OEP)(PMS)(NO)]^+$ in Table 4 have also been shown not to have any unusual nitrosyl interactions.[49]

(49) Ellison, M. K.; Scheidt, W. R., unpublished structural observations.

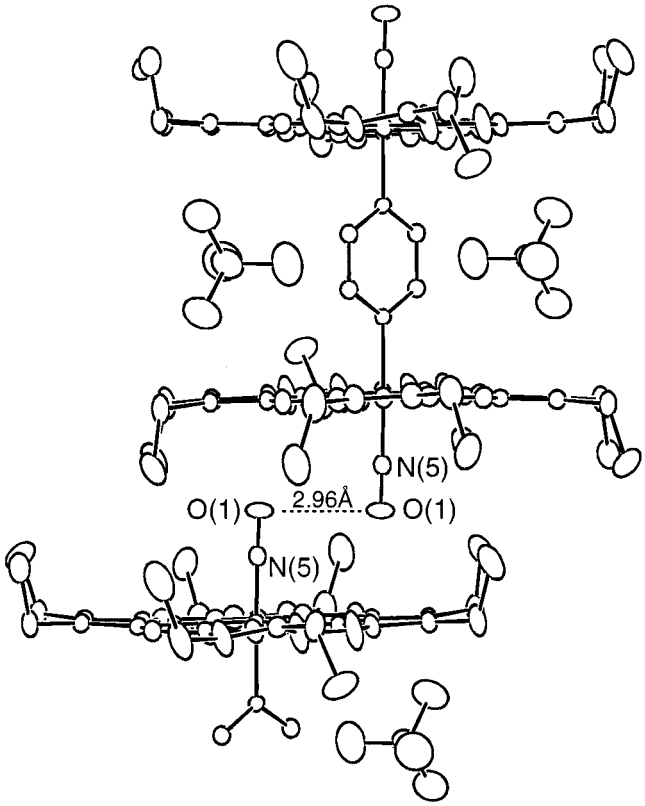

Figure 9. ORTEP diagram illustrating the interacting nitrosyls of the $\{[Fe(OEP)(NO)]_2Prz\}(ClO_4)_2$ system. The solvent molecules and hydrogen atoms have been omitted for clarity. The two closely approaching nitrosyls are related by an inversion center.

In the $\{FeNO\}^7$ systems, the addition of the sixth ligand increases the ligand field splitting and increases the electron density at the iron center. This in turn leads to increased donation from iron to the π^* orbital of NO and hence to a decrease in the N−O bond strength. The same effect might have been expected in the $(FeNO\}^6$ porphyrin complexes, but the frequency pattern difference is consistent with decreased donation from iron to the π^* orbitals of NO. In this case, an increased ligand field must depress the energy of the metal d_π's, and lead to poorer energy matching and hence decreased donation from iron to the π^* orbital of NO. However, the nearly invariant values of the $Fe-N_{NO}$ bond distance as a function of coordination number in both the $\{FeNO\}^6$ and $\{FeNO\}^7$ species suggests that the difference in π bonding as coordination number is changed is not large and emphasizes the importance of considering M−N−O as a strongly delocalized entity and the importance of the electron count in the $\{MNO\}^n$ unit in defining the structure.[8,9]

Summary. We have shown that it is possible to prepare and isolate six-coordinate $\{FeNO\}^6$ species as crystalline solids. Success depends on maintaining an NO atmosphere during the crystallization/isolation procedure and by avoiding conditions where nucleophilic attack on the $[Fe-NO]^+$ unit leads to reductive nitrosylation. All complexes display structural features consistent with a low-spin state and short $Fe-N_{NO}$ bond lengths. All of the axial Fe−N bond distances trans to the nitrosyl ligand are normal. We have shown by the structural and spectroscopic data reported herein that there is a clear distinction between $\{FeNO\}^6$ and $\{FeNO\}^7$ species. Such distinctions should be especially useful for identifying native nitrosyl proteins and reactive intermediates.

Acknowledgment. We thank the National Institutes of Health for support of this research under Grant GM-38401 to W.R.S. Funds for the purchase of the FAST area detector diffractometer was provided through NIH Grant RR-06709 to the University of Notre Dame. We thank Prof. John Enemark for stimulating discussions on vibrational spectroscopy of the NO complexes.

Supporting Information Available: Tables S1−S36, giving complete crystallographic details, atomic coordinates, bond distances and angles, anisotropic temperature factors, and fixed hydrogen atom positions for all six structures. Figures S1 and S2 include formal diagrams of the porphinato core for $[Fe(OEP)(Prz)(NO)]ClO_4$ and $[Fe(OEP)(Pz)(NO)]ClO_4$ (**2**). Figure S3 illustrates the types of core distortions found in porphyrin species (PDF). An X-ray crystallographic file, in CIF format, is available. This material is available free of charge via the Internet at http://pubs.acs.org.

JA984308Q